

Imaging cortical correlates of illusion in early visual cortex

Dirk Jancke, Frédéric Chavane, Shmuel Naaman & Amiram Grinvald

Department of Neurobiology and the Grodetsky Center for Studies of Higher Brain Function, The Weizmann Institute of Science, 76100 Rehovot, Israel

Exploring visual illusions reveals fundamental principles of cortical processing. Illusory motion perception of non-moving stimuli was described almost a century ago by Gestalt psychologists^{1,2}. However, the underlying neuronal mechanisms remain unknown. To explore cortical mechanisms underlying the ‘line-motion’ illusion³, we used real-time optical imaging^{4–6}, which is highly sensitive to subthreshold activity. We examined, in the visual cortex of the anaesthetized cat, responses to five stimuli: a stationary small square and a long bar; a moving square; a drawn-out bar; and the well-known line-motion illusion³, a stationary square briefly preceding a long stationary bar presentation. Whereas flashing the bar alone evoked the expected localized,

short latency and high amplitude activity patterns^{7,8}, presenting a square 60–100 ms before a bar induced the dynamic activity patterns resembling that of fast movement. The preceding square, even though physically non-moving, created gradually propagating subthreshold cortical activity that must contribute to illusory motion, because it was indistinguishable from cortical representations of real motion in this area. These findings demonstrate the effect of spatio-temporal patterns of subthreshold synaptic potentials on cortical processing and the shaping of perception.

Almost a century ago, Wertheimer¹ and Kenkel² made the striking observation that non-moving stimuli can give rise to motion perception⁹. Assuming that the facilitatory effect of the cue spread gradually in space and time^{10–12}, the sensation of motion evoked by a subsequently flashed bar during the line-motion illusion³ could result from sequential suprathreshold activation, thus mimicking real motion drawing away from the local cue^{3,13} (Fig. 1a, b; Supplementary movie SI 1, page 1). Whereas the findings of several psychophysical studies implicate top-down involvement of higher cortical areas^{14–16}, others argue for bottom-up (that is, stimulus induced) mechanisms occurring at early processing stages^{16–18}. In none of those studies, however, were the neurophysiological

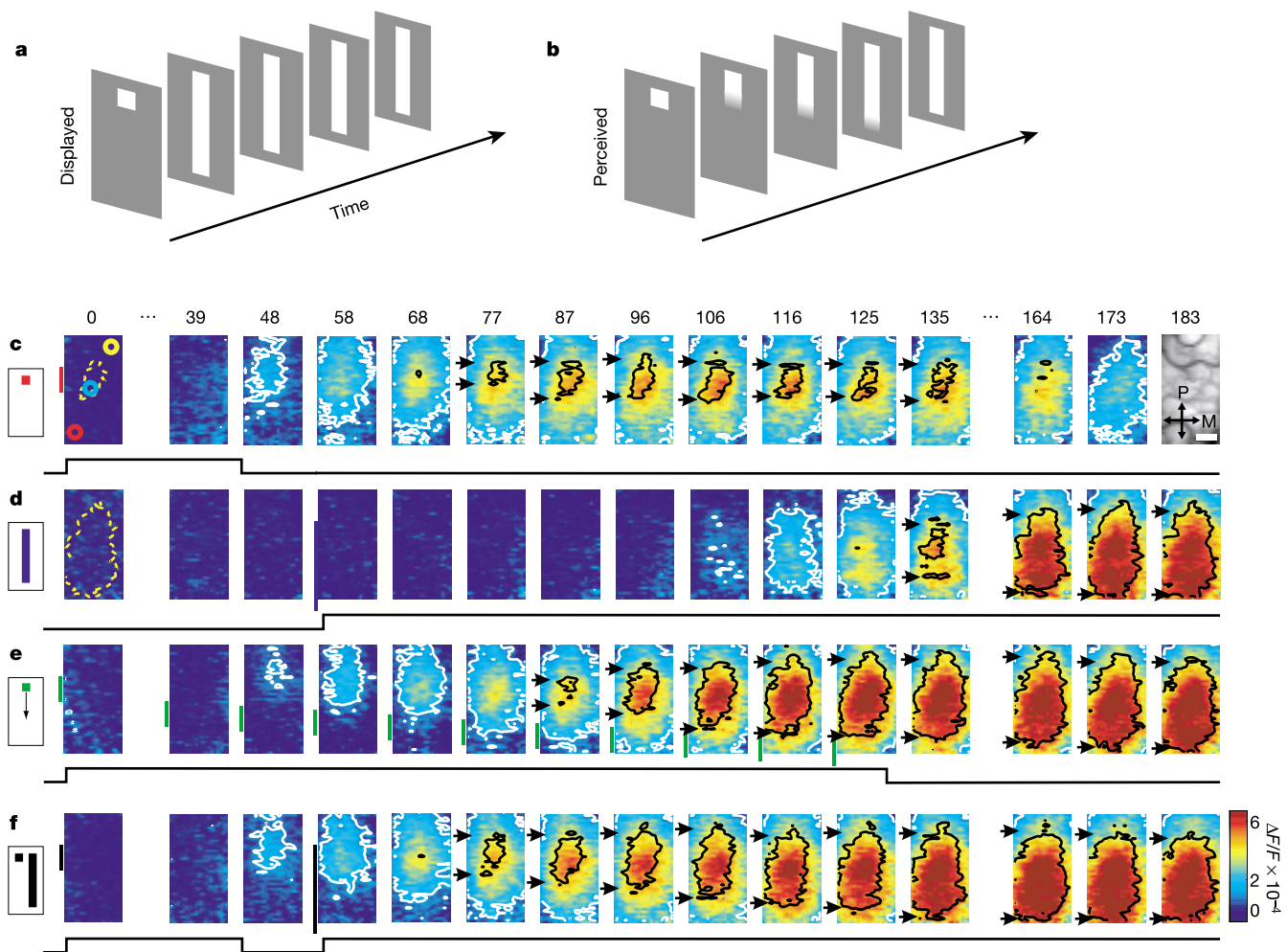


Figure 1 Cortical representations of stationary, moving, and illusory moving stimuli. The line-motion illusion. **a**, Square (‘cue’) presented before a bar stimulus. **b**, Subjects report illusory line-drawing. See Supplementary movie SI 1, page 1. **c–f**, Patterns of evoked cortical activity as a function of time. Yellow dotted contours approximate retinotopic representation of the stimuli; coloured circles indicate extracellular recording sites. White contours delimit low-amplitude activity (significance level; $P < 0.05$). The cortical area

imaged is shown at upper right. Scale bar, 1 mm; P, posterior; M, medial. Green vertical lines in **e** indicate estimated position of the stimuli along posterior–anterior axis. Time in milliseconds after stimulus onset is shown at the top. Stimulation time is shown at the bottom of each row. Colour scale indicates averaged fractional changes in fluorescence intensity ($\Delta F/F$). Stimuli: **c**, flashed small square. **d**, Flashed bar. **e**, Moving small square (32° s^{-1}). **f**, Line-motion paradigm. 22 repetitions were averaged.

mechanisms creating such illusory motion examined directly.

To identify neuronal mechanisms that produce illusory motion, we employed voltage-sensitive dye (VSD) imaging⁴ that allows sensitive monitoring of the changes in membrane potential, and particularly sub- and suprathreshold synaptic potentials^{4,19–21}, with high spatial and temporal resolutions⁶. Figure 1c depicts the cortical VSD response evoked by the cue alone (small square). As the VSD signal is sensitive primarily to synaptic potentials rather than to spikes^{19–21}, we searched for a way to delineate the spiking regions in the resulting optical maps. From basic principles of the retinotopic (spiking) organization of area 18, and because of the known spread of subthreshold synaptic potentials far beyond that area^{4,5,21}, it was obvious that the spiking region should be located in the area of high VSD amplitudes. Therefore, the dynamic behaviour of evoked low- and high-amplitude activity was analysed separately. Low-amplitude activity spread far beyond the retinotopic representation of the square, at 0.09 m s^{-1} ($n = 19$), consistent with conduction velocity along horizontal connections^{5,22}. In contrast, high-amplitude activity (encircled by black contours) showed negligible lateral extension (Fig. 1c arrows), after an initial $\sim 20 \text{ ms}$ period of spread. Single-unit recordings (coloured circles; Fig. 1c, first frame) showed that spiking activity evoked by the square was limited to the high-amplitude area (Fig. 2a, b, discussed below). The second stationary stimulus, the bar flashed alone 60 ms later, yielded a similar finding (Fig. 1d). High-level activity delineated a circumscribed region representing the elongated shape of the bar almost at once (arrows). In addition, activity within this cortical region consistently had the shortest latencies (34–37 ms; Supplementary Fig. SI 2).

To examine how actual motion is represented across the imaged cortical area, the small square was moved across exactly the same region as that covered by the bar (Fig. 1e). We again observed a rapid

spread of low-amplitude activity. However, in contrast to the stationary conditions, the moving square evoked high-amplitude activity propagating anteriorly, reflecting the motion trajectory of the square (lower arrows; Supplementary Fig. SI 3 for squares moving at different speeds and electrophysiological recordings). In summary, these findings suggest that regions of high optical activity correspond to the spiking representations of the stimuli. We therefore refer to those cortical regions as ‘spike discharge’ (SD) zones.

Next, we investigated the spatio-temporal pattern of activity evoked by the Hikosaka³ line motion paradigm (Fig. 1f). In contrast to the conditions in which either the square or the bar was flashed alone, the SD zone did not remain stable but was gradually drawn out towards the end of the cortical bar representation (lower arrows). Thus, although these two stimuli were stationary, the anterior portion of the high-activity region propagated similarly to the moving stimulus (Fig. 1e), suggesting that cortical correlates of illusory line motion were directly visualized here (Supplementary movie SI 1, page 2; another example in Supplementary Fig. SI 4).

To verify this suggestion, we imaged the responses to stimuli that were drawn out to full bar length at a speed of 32° s^{-1} , thus mimicking the perceived illusory motion (Fig. 2). The spatio-temporal patterns evoked by this high-speed real motion closely resembled the activity induced by the line-motion stimuli (Fig. 2a, second and third rows). The link between such cortical spatio-temporal patterns and object physical speeds is shown in a subsequent experiment where the bar was drawn out more slowly (16° s^{-1} , fourth row Fig. 2a). In this case, the speed of propagating SD activity was slower than for line motion, demonstrating that the expanding SD zone carries information about motion

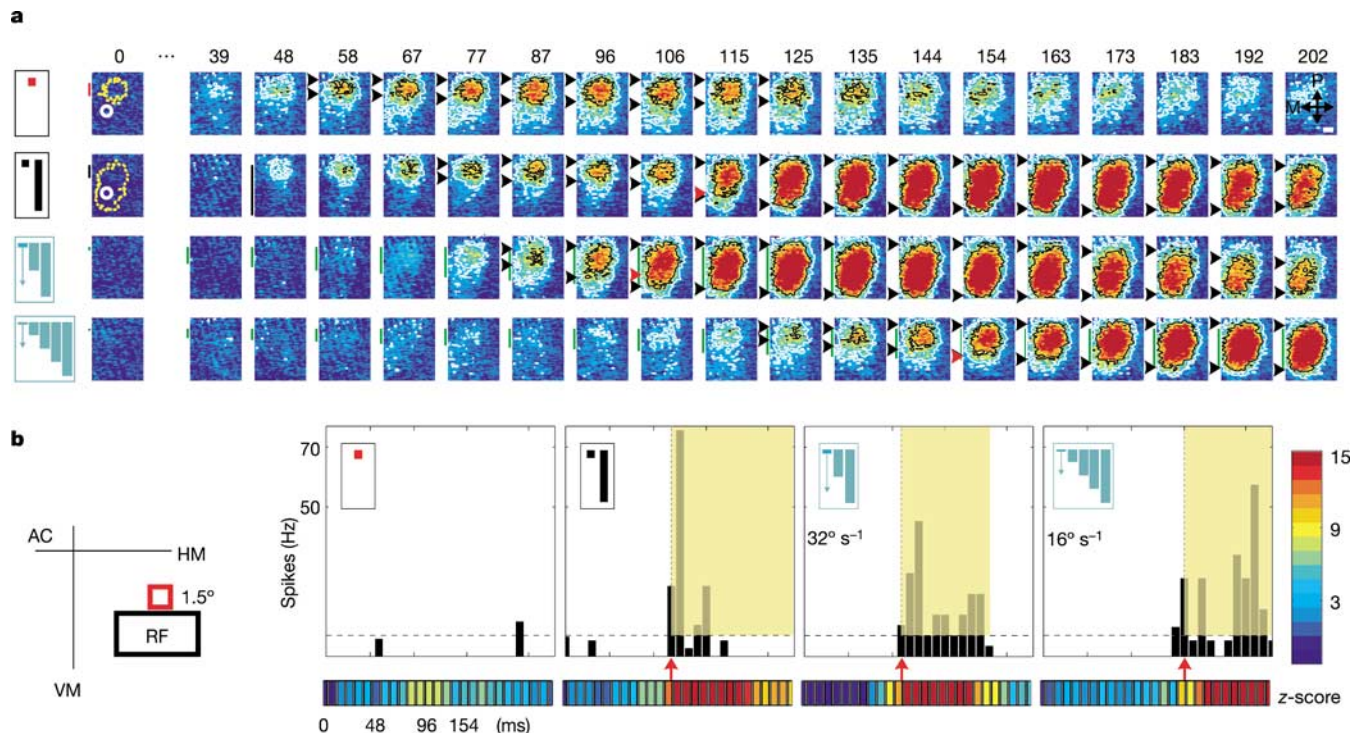


Figure 2 Both illusory and real motion evoke propagating spiking discharge (SD) zones. **a**, From top to bottom: VSD images patterns of activity evoked by flashed square, line-motion, and drawn-out bar at 32° s^{-1} and 16° s^{-1} . Multi-unit spiking activity was recorded simultaneously at the location marked by the white circle at frame 0; yellow dotted contours at frame 0 approximate sizes of the SD zone representing square and bar (left). **b**, The neurons' receptive field at the bottom left (RF, black), stimulus position and size (red); VM, HM, vertical, horizontal meridian; AC, area centralis; PSTHs of spiking

responses to the respective SD conditions are on the right. Dashed line depicts significance ($z\text{-score} = 2$; 32 repetitions). Spikes are detected as soon as activity reaches the SD threshold at the position of the electrode (red arrows). Bottom shows $z\text{-scores}$ of the VSD signal at electrode position. Area in yellow depicts the period in which the optical signal at the extracellular recording site is above SD level as shown by the three red triangles in the VSD patterns (**a**).

speed. Simultaneous VSD imaging and multi-unit recordings again confirmed that the SD zone corresponded to cortical regions containing propagating suprathreshold (spiking) activity whereas activity outside its border was subthreshold (Fig. 2b).

To specify the differences in the cortical representations of the various stimuli, we examined the time courses of activity in three contiguous regions of interest (ROIs; squares in insets of Fig. 3a). Activity evoked by the flashed square alone (red) was detected at all sites, but was smaller and slower at more anterior cortical positions. In sharp contrast, the flashed bar alone (blue) evoked activities exhibiting identical latencies and amplitudes within all three ROIs. Evidently, the two lower ROIs were outside the retinotopically activated area for the square and inside for the bar, containing activity that reached the SD level for many neurons (marked in yellow). The responses to the moving square, at the three ROIs, passed the SD level at consecutive times, thus representing the motion (green, Fig. 3b). Figure 3c shows the time course of activity evoked by the line-motion stimulus (black). As expected, at response onset the responses were similar to those evoked by the cue alone (compare black and red). However, during the time interval when the response to the stationary square alone turned into a plateau, activity for the line-motion stimuli continued to rise, crossing SD level at successive times, just as observed for motion. The latency of the response to the subsequently presented bar was strikingly shorter than the response to the bar alone (arrow in Fig. 3c, ~18 ms). Similar results were obtained in other experiments (23 ± 6 ms, mean \pm s.d., $n = 4$), underscoring the impact of sub-threshold activity on time of spiking evoked by a subsequent stimulus.

To further characterize the nature of the synaptic interactions between activities evoked by the cue stimulus and the bar response, we compared the time course of line-motion evoked activity with the calculated linear combination of its two components presented alone. The traces in Fig. 3d show the measured (black) and the calculated responses (pink), revealing two deviations from linearity of synaptic interactions. Activity was first increased by 17% (other

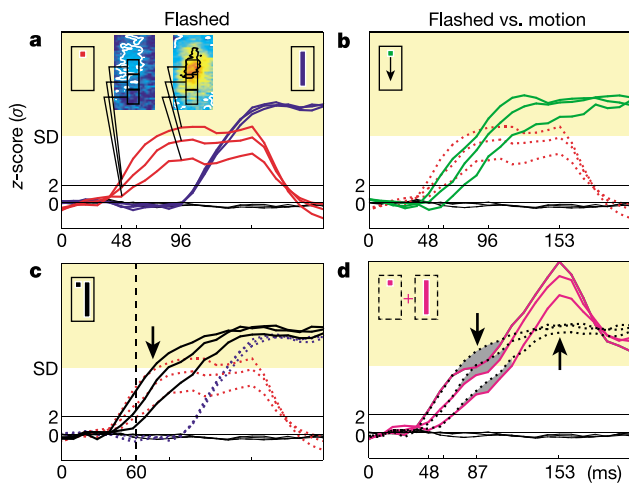


Figure 3 Time course of activity evoked by the stationary bar is largely affected by the preceding stationary cue. Responses from three contiguous cortical regions of interest (ROIs, black rectangles in insets at top). Yellow area marks activity above SD level; significance level ($z\text{-score} = 2$) is shown by a horizontal black line. **a**, Small square (red), bar (blue). **b**, Moving square (green; 32° s^{-1}), flashed square (red). **c**, Flashed square (red), flashed bar (blue), and line-motion condition (black). Arrow points to short latency of the response to the subsequently flashed bar; vertical dashed line shows time of presentation. **d**, Linear superposition of responses evoked by square and bar alone (pink) compared with the line-motion condition (black). Grey areas outline early deviation from a linear response. Thin black traces in **a–d** show time courses of blank conditions, indicating the excellent signal to noise ratio obtained.

experiments: $24 \pm 10\%$, mean \pm s.d.; $n = 4$), and ~ 50 ms later, activity was decreased by as much as 32% ($31 \pm 4\%$; $n = 4$). An increase in the VSD signal could either reflect increase in excitation or withdrawal of inhibition. The net effect appeared ‘facilitatory’ in the early response phase whereas overall ‘suppression’ dominated at later times^{12,23,24}.

Do the characteristics of cortical subthreshold spread account for the illusory motion? Level of activation and speed of propagation of subthreshold activity co-varied: the higher the activation, the slower the propagation speed (Fig. 4a). This could arise from a gradual increase in inhibition²³, or from a gradual decrease in the synaptic density/efficacy of horizontal projections at further intracortical distances^{25,26}. The velocity of the subthreshold spread evoked by the cue was found to be similar to the velocity of SD activity produced when the line-motion stimuli are presented (Fig. 4b). It is therefore not a coincidence that propagating activity representing illusory motion was similar to SD activity evoked by real bar drawing or a moving square at a very specific speed (Fig. 4c). In contrast, no SD propagation was produced by a stationary bar or square alone (Fig. 4d; see Supplementary Information SI 5). Changing cue characteristics altered spatio-temporal patterns in a way consistent with psychophysical studies: first, when flashing a square with lower luminance the threshold for SD activity was reached later (Fig. 4e; Supplementary Fig. SI 6), in line with a weaker percept of illusory line motion¹³. Second, motion was not observed when the delay between the preceding square and the following bar exceeded 350 ms (Fig. 4f). Third, no line-motion correlates were found for spatial distances between square and bar beyond 6° in the visual field (not shown). Altogether, these findings confirmed the spatio-temporal limits of low-level processes participating in illusory line motion as demonstrated psychophysically^{16–18}. We therefore suggest that characteristics of subthreshold spread in early visual

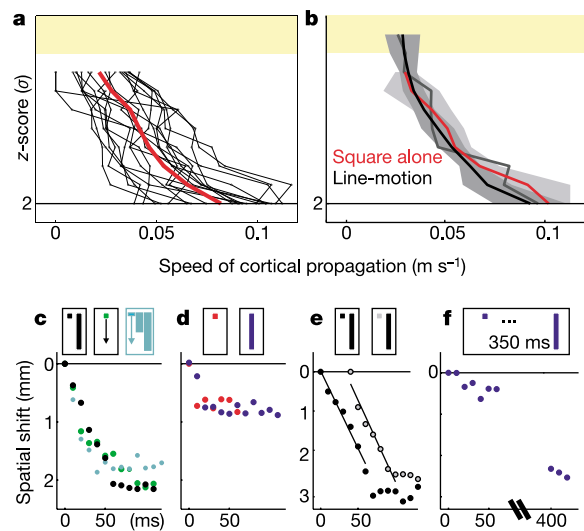


Figure 4 SD activity propagates only when real or illusory motion occurs. **a, b**, Deceleration of propagation speed with increasing amplitudes (see Methods). **a**, Speeds of propagation for flashed squares (17 hemispheres), red trace shows average. Evidently, for the stationary square, no speed exists above SD activity level (yellow). **b**, Line motion (black) compared to the square alone (red; across four experiments). A square of lower luminance (see Methods) does not change propagation speed (grey line, 33 repetitions). Above SD level, responses to the line motion paradigm continue propagating at similar speed. **c–f**, Propagation of the SD zone (see Methods). **c**, Propagation of SD activity is evident for line motion (black), the moving square (green), and bar drawing (cyan). **d**, After an initial small expansion, no shift is observed for the flashed-stationary square and bar alone (red, blue). **e**, Reducing the square’s contrast (grey) causes a lagged start of line motion. **f**, An interval of 350 ms between square and bar shows no line-motion effect; no SD activity is detectable at 70–400 ms.

areas shown here are cortical correlates of the bottom-up mechanism underlying the line-motion illusion, without need of attention^{18,27–29}.

It has been reported that when multiple inducers (or different stimulus features like colour, contrast, or texture) are used there is evidence for a second, top-down component that operates on a slower timescale^{16,18,30}. Furthermore, the illusory line motion can be modulated by attention²⁹ or can be voluntarily induced by non-retinotopic mechanisms¹⁶ even across sensory modalities¹⁵ (but see ref. 29, and Supplementary Information SI 7). Such controversies in psychophysical studies underscore the importance of physiological measurements. These top-down processing and attentional mechanisms^{14–16,29} remain to be explored in behaving subjects, by bringing together psychophysics and fast functional imaging. As onset of any stimulus will create an intricate spatio-temporal pattern of spreading subthreshold synaptic activity, we conclude that subthreshold synaptic spread must serve a fundamental processing strategy that strongly affects the spatio-temporal integration of any natural sensory input. □

Methods

Animals

All surgical and experimental procedures were in accordance with NIH guidelines. Details are described elsewhere⁶. Briefly, recordings were performed in 15 adult cats, initially anaesthetized with ketamine (15 mg kg⁻¹) and xylazine (1 mg kg⁻¹), supplemented with atropine (0.05 mg kg⁻¹). After tracheotomy, cats were artificially respired and were anaesthetized with 1–1.5% halothane (0.8–1% during recordings) in a 1:1 mixture of O₂ and N₂O. The skull was opened above area 18 and the dura was resected. Paralysis was induced with pancuronium bromide (0.2 mg kg⁻¹ h⁻¹, intravenously). The eyes were covered with zero-power smooth contact lenses. External lenses were used to focus the eyes on the screen. Eyes were converged using a prism in front of the eye ipsilateral to the recorded hemisphere. To control for eye drift, the position of the area centralis was repeatedly measured. Eye movements were completely eliminated under these experimental conditions.

Stimulation, imaging and electrical recordings

The cortex was stained for 2.5–3 h using the oxonol dye RH-1691. A FUJIX HR Deltaron 1700 camera was used for data acquisition. Combined intracellular recordings and VSD imaging *in vivo* have demonstrated that the VSD signal reports amplitude, direction, and propagation speed of synaptic potentials in layer 2/3 of cortical neurons^{20,21} (in a linear fashion, without saturation). Details of the method have been previously described⁶. Stimuli were displayed binocularly with the VSG series 3 (Cambridge Research Systems) on a monitor located 57 cm from the cat's eyes, at a refresh rate of 150 Hz. The achromatic luminance of the stimuli was 52.5 cd m⁻² (26.2 cd m⁻² when testing for lower luminance). Stimuli were presented on a grey background (10.5 cd m⁻²). Small squares of light were flashed for 50 ms, and their locations on the screen were determined according to single-unit recordings. Flash duration of the vertical flashed bar was 130 ms. Varying the cue lead times between 60 and 100 ms did not significantly alter propagation speed, in accordance with psychophysical studies pointing to a stable illusory line motion within the same range of bar delays^{3,17,18}. Hikosaka *et al.*³ report the strongest illusion when presenting an inducing cue 100–200 ms before flashing a line. Von Grünau *et al.*¹⁸ discriminate two contributions to illusory line-motion: a pre-attentive fast-acting process^{16,30} followed by a slower, probably top-down process, showing strongest motion effects for bars presented 200–300 ms after the cue. Therefore, to test the limits of line-motion induction, we increased the bar delay up to 350 ms and presented the bar separated by 3–6° from the square. Stimuli were located between 4° and 5.5° eccentricity in different experiments and were presented pseudo-randomly. Single-unit and multi-unit recordings were performed as described elsewhere^{7,8}. A recording time of about 1 min surrounded each stimulus presentation.

Data analysis

To remove slow common noise, we obtained the time courses of evoked activity by subtracting the average value at each pixel before stimulus onset from each pixel value. To correct for the fast heart beat noise and respiration noise and to obtain the activation maps (in units of fractional change of fluorescence intensity $\Delta F/F$), we divided the resulting values by the activity recorded during the 'no-stimulus' condition⁶. Such data reflect evoked population neuronal activity, as confirmed by intracellular recordings^{19,20}.

As shown by the black traces in Fig. 3a–d, the signal to noise ratio in these VSD experiments is excellent. To calculate statistical significance (*z*-score), we divided each pixel by its standard deviation calculated over the blank conditions, after subtracting its mean. No spatio-temporal filters were used. We computed the speeds of cortical activity within space–time diagrams across the entire time courses of the evoked responses. Activity was averaged for each single time frame across the *x*-dimension, providing us with a single space dimension as a function of time (space–time diagram). Contours were calculated at 10 different *z*-score levels of activity (scaled in steps of 10% from a *z*-score of 2 to the maximum *z*-score observed) on such diagrams. The slope of each contour (computed by linear regression) within such a space–time diagram corresponds to the speed of propagating activity at a given *z*-score.

Received 26 November 2003; accepted 5 February 2004; doi:10.1038/nature02396.

- Wertheimer, M. Experimentelle Studien über das Sehen von Bewegung. *Z. Psychol.* **61**, 161–265 (1912).
- Kenkel, F. Untersuchungen über den Zusammenhang zwischen Erscheinungsgröße und Erscheinungsbewegung bei einigen sogenannten optischen Täuschungen. *Z. Psychol.* **67**, 358–449 (1913).
- Hikosaka, O., Miyauchi, S. & Shimojo, S. Focal visual attention produces illusory temporal order and motion sensation. *Vision Res.* **33**, 1219–1240 (1993).
- Grinvald, A., Anglister, L., Freeman, J. A., Hildesheim, R. & Manker, A. Real-time optical imaging of naturally evoked electrical activity in intact frog brain. *Nature* **308**, 848–850 (1984).
- Grinvald, A., Lieke, E., Frostig, R. & Hildesheim, R. Cortical point-spread function and long-range lateral interactions revealed by real-time optical imaging of macaque monkey primary visual cortex. *J. Neurosci.* **14**, 2545–2568 (1994).
- Shoham, D. *et al.* Imaging cortical dynamics at high spatial and temporal resolution with novel blue voltage-sensitive dyes. *Neuron* **24**, 791–802 (1999).
- Albus, K. A quantitative study of the projection area of the central and the paracentral visual field in area 17 of the cat. I. The precision of the topography. *Exp. Brain Res.* **24**, 159–179 (1975).
- Tusa, R. J., Rosenquist, A. C. & Palmer, L. A. Retinotopic organization of areas 18 and 19 in the cat. *J. Comp. Neurol.* **185**, 657–678 (1979).
- Kanizsa, G. Sulla polarizzazione del movimento gamma. *Arch. Psicol. Neurol. Psichiatr.* **3**, 224–267 (1951).
- Posner, M. I., Snyder, C. R. R. & Davidson, B. J. Attention and the detection of signals. *J. Exp. Psychol.* **109**, 160–174 (1980).
- Sagi, D. & Julesz, B. Enhanced detection in the aperture of focal attention during simple discrimination tasks. *Nature* **321**, 693–695 (1986).
- Polat, U., Mizobe, K., Pettet, M. W., Kasamatsu, T. & Norcia, A. M. Collinear stimuli regulate visual responses depending on cell's contrast threshold. *Nature* **391**, 580–584 (1998).
- von Grünau, M., Racette, L. & Kwas, M. Measuring the attentional speed-up in the motion induction effect. *Vision Res.* **36**, 2433–2446 (1996).
- von Grünau, M. & Faubert, J. Intraattribute and interattribute motion induction. *Perception* **23**, 913–928 (1994).
- Shimojo, S., Miyauchi, S. & Hikosaka, O. Visual motion sensation yielded by non-visually driven attention. *Vision Res.* **37**, 1575–1580 (1997).
- Hikosaka, O. & Miyauchi, S. Voluntary and stimulus induced attention detected as motion sensation. *Perception* **22**, 517–526 (1993).
- Steinman, B. A., Steinman, S. B. & Lehmkuhle, S. Visual attention mechanisms show a center-surround organization. *Vision Res.* **35**, 1859–1869 (1995).
- von Grünau, M., Dube, S. & Kwas, M. Two contributions of motion induction: a preattentive effect and facilitation due to attentional capture. *Vision Res.* **36**, 2447–2457 (1996).
- Sterkin, A. *et al.* Real-time optical imaging in cat visual cortex exhibits high similarity to intracellular activity. *Neurosci. Lett.* **51**, S41–S41 (1998).
- Grinvald, A. *et al.* in *Modern Techniques in Neuroscience Research* (eds Windhorst, U. & Johansson, H.) 893–969 (Springer, New York, 1999).
- Petersen, C., Grinvald, A. & Sakmann, B. Spatiotemporal dynamics of sensory responses in layer 2/3 of rat barrel cortex measured *in vivo* by voltage-sensitive dye imaging combined with whole-cell voltage recordings and neuron reconstructions. *J. Neurosci.* **23**, 1298–1309 (2003).
- Bringuiet, V., Chavane, F., Glaeser, L. & Frégnac, Y. Horizontal propagation of visual activity in the synaptic integration field of area 17 neurons. *Science* **283**, 695–699 (1999).
- Hirsch, J. A. & Gilbert, C. D. Synaptic physiology of horizontal connections in the cat's visual cortex. *J. Neurosci.* **11**, 1800–1809 (1991).
- Jancke, D. *et al.* Parametric representation of retinal location: Neural population dynamics and interaction in cat visual cortex. *J. Neurosci.* **19**, 9016–9028 (1999).
- Kisvárdy, Z. F., Toth, E., Rausch, M. & Eysel, U. T. Orientation-specific relationship between populations of excitatory and inhibitory lateral connections in the visual cortex of the cat. *Cereb. Cortex* **7**, 605–618 (1997).
- Seriès, P., Georges, S., Lorenceau, J. & Frégnac, Y. Orientation dependent modulation of apparent speed: a model based on the dynamics of feed-forward and horizontal connectivity in V1 cortex. *Vision Res.* **42**, 2781–2797 (2002).
- Kawahara, J., Yokosawa, K., Nishida, S. & Sato, T. Illusory line motion in visual search: Attentional facilitation or apparent motion? *Perception* **25**, 901–920 (1996).
- Cavanagh, P., Arguin, M. & von Grünau, M. Interattribute apparent motion. *Vision Res.* **29**, 1197–1204 (1989).
- Downing, P. E. & Treisman, A. M. The line-motion illusion: Attention or implosion? *J. Exp. Psychol. Hum. Percept. Perform.* **23**, 768–779 (1997).
- Nakayama, K. & Mackeben, M. Sustained and transient components of focal visual attention. *Vision Res.* **29**, 1631–1647 (1989).

Supplementary Information accompanies the paper on www.nature.com/nature.

Acknowledgements We thank R. Hildesheim for synthesizing the dye, RH-1692; C. Wijnbergen, D. Ettner and Y. Toledo for technical assistance; I. Lampl for programming the spike recording software; and A. Arieli, A. Gupta, C. E. Schreiner, D. Sharon, D. Sagi, E. Seidemann, H. Slovlin, I. Vanzetta, S. Ullman and Y. Frégnac for comments and discussions. This work was supported by the Grodzky Center, the Goldsmith, Korber and ISF Foundations and a BMBF/MOS and NIH grants (to A.G.). D.J. was supported by the Minerva Foundation, Germany, and F.C. by a Marie Curie EU fellowship.

Competing interests statement The authors declare that they have no competing financial interests.

Correspondence and requests for materials should be addressed to D.J. (jancke@neurobiologie.ruhr-uni-bochum.de).